Cerebral Cortex January 2013;23:148–161
doi:10.1093/cercor/bhr390
Advance Access publication January 30, 2012

Layer-Specific Modulation of the Prefrontal Cortex by Nicotinic Acetylcholine Receptors

Rogier B. Poorthuis, Bernard Bloem, Benita Schak, Jordi Wester, Christiaan P. J. de Kock and Huibert D. Mansvelder

Department of Integrative Neurophysiology, Center for Neurogenomics and Cognitive Research, Neuroscience Campus Amsterdam, VU University, 1081HV Amsterdam, the Netherlands

Rogier B. Poorthuis and Bernard Bloem share first authorship.

Address correspondence to email: huibert.mansvelder@cncr.vu.nl.

Acetylcholine signaling through nicotinic receptors (nAChRs) in the prefrontal cortex (PFC) is crucial for attention. Nicotinic AChRs are expressed on glutamatergic inputs to layer V (LV) cells and on LV interneurons and LVI pyramidal neurons. Whether PFC layers are activated by nAChRs to a similar extent or whether there is layer-specific activation is not known. Here, we investigate nAChR modulation of all PFC layers and find marked layer specificity for pyramidal neurons: LII/III pyramidal neurons and glutamatergic inputs to these cells do not contain nAChRs, LV and LVI pyramidal neurons are modulated by α7 and β2* nAChRs, respectively. Interneurons across layers contain mixed combinations of nAChRs. We then tested the hypothesis that nAChRs activate the PFC in a layer-specific manner using 2-photon population imaging. In all layers, nAChR-induced neuronal firing was dominated by β2* nAChRs. In LII/III, only interneurons were activated. In LV and LVI, both interneurons and pyramidal neurons were activated, the latter most strongly in LVI. Together, these results suggest that in the PFC nAChR activation results in inhibition of LII/III pyramidal neurons. In LV and LVI, nAChR-induced activation of inhibitory and excitatory neurons results in a net augmentation of output neuron activity.

Keywords: acetylcholine, cortical layers, network, nicotinic acetylcholine receptor, prefrontal cortex

Introduction

The prefrontal cortex (PFC) plays a central role in attention (Groenewegen and Uylings 2000; Dalley, Cardinal, et al. 2004). Acetylcholine critically modulates the PFC during attention behavior (Passetti et al. 2000; Dalley, Theobald, et al. 2004; Parikh et al. 2007) and shows rapid phasic dynamics on a seconds timescale (Parikh et al. 2007; Sarter et al. 2009). Nicotinic acetylcholine receptors (nAChRs), a subset of cholinergic receptors, are fast ionotropic receptors and their activation kinetics suggests that they are efficiently activated by these rapid increases in acetylcholine. Supporting this, mice lacking specific subunits of the nAChR show a decrement in attention performance (Young et al. 2007; Bailey et al. 2010), and reexpression of the β2 subunit in the PFC improves attention of β2-null mice (Guillem et al. 2011). In addition, nicotinic receptor agonists acting on the PFC increase performance on these tasks (Hahn et al. 2003; Howe et al. 2010). To understand the role of nAChRs in cognitive functioning, it is crucial to determine how nAChRs alter cortical information processing at the cellular and network level. Here, we investigate what the relative impact of nAChR stimulation is on activity in different layers of the PFC network.

Neuronal network activation will strongly depend on which cell types express nAChRs as well as the subunit composition of the receptor. Pyramidal neurons in layer VI of the PFC contain β2* nAChR accompanied by the accessory α5 subunit, and these receptors activate output neurons that project to the medial dorsal thalamus (Kassam et al. 2008). Layer V pyramidal neurons are excited by nAChRs that enhance glutamatergic inputs through stimulation of presynaptic β2* nAChRs. nAChR modulation of glutamatergic inputs was abolished by lesioning the medial dorsal thalamus, showing that excitatory inputs from the medial dorsal thalamus to the PFC are specifically augmented by β2* nAChRs (Lambe et al. 2003). nAChRs also increase inhibition to layer V pyramidal neurons (Couey et al. 2007). In layer V regular-spiking nonpyramidal cells and low-threshold spiking cells express α7 and β2* nAChRs, whereas fast-spiking (FS) interneurons do not. In addition, low-threshold and FS interneurons are stimulated through presynaptic nAChRs on glutamatergic inputs (Couey et al. 2007; Poorthuis et al. 2009). What type of synaptic inputs and neurons in layer II/III are regulated by nAChRs is not known. It is also unknown whether layer VI interneurons are modulated by nAChRs. In this study, we address these issues. In addition, since nAChRs are found on both inhibitory and excitatory neurons in different PFC layers, it is not straightforward to predict how action potential firing of PFC output neurons is altered by nAChR stimulation. The nAChR distribution in the PFC suggests a layer-specific activation of the PFC by nAChRs. To test this hypothesis, we used 2-photon calcium imaging of large-scale PFC neuronal networks with single-cell resolution to assess how nAChR-induced activity is distributed across different layers. We find that nAChR-induced neuronal activity increases with depth in the cortex and is markedly different across PFC layers due to specific distribution of β2* nAChRs.

Materials and Methods

Prefrontal Cortical Slice Preparation

Prefrontal coronal cortical slices (300 μm) were prepared from postnatal day 14 (P14) to P21 C57 BL/6 mice, in accordance with institutional and Dutch license procedures. Following rapid decapitation, the brain was removed from the skull in ice-cold artificial cerebrospinal fluid (ACSF) containing 125 mM NaCl, 3 mM KCl, 1.25 mM NaH_2PO_4, 3 mM $MgSO_4$, 1 mM $CaCl_2$, 26 mM $NaHCO3$, and 10 mM glucose (~300 mOsm). After removal of the cerebellum, the brain was glued on this plane to create a coronal orientation for cutting slices. Slices were then transferred into holding chambers containing ACSF 125 mM NaCl, 3 mM KCl, 1.25 mM NaH_2PO_4, 1 mM $MgSO_4$, 2 mM $CaCl_2$, 26 mM $NaHCO_3$, and 10 mM glucose (~300 mOsm) and bubbled with carbogen gas (95% O_2/5% CO_2) to recover for at least an hour.

Electrophysiology

Slices were transferred to the recording chamber and perfused with standard ACSF (2–3 mL/min). All experiments were performed at 31–34 °C. Cells were visualized using differential interference contrast microscopy. Recordings were made using Multiclamp 700B amplifiers (Axon Instruments, CA), sampled at a frequency of 20 kHz, digitized by the pClamp software (Axon), and later analyzed off-line. Patch pipettes (3–5 MOhm) were pulled from standard-wall borosilicate capillaries and

were filled with intracellular solution: 140 mM K-gluconate, 1 mM KCl, 10 mM 4-(2-hydroxyethyl)-1-piperazineethanesulfonic acid, 4 mM K-phosphocreatine, 4 mM ATP-Mg, and 0.4 mM GTP (pH 7.2–7.3, pH adjusted to 7.3 with KOH) (290–300 mOsm) and biocytin (4 mg/mL) (used for excitatory postsynaptic current [EPSC] and puff application experiments, reversal potential chloride ~−127 mV, hence, inhibitory postsynaptic currents [IPSCs] in this case are detected as outward currents). Action potential profiles of cells were made using hyperpolarizing and depolarizing current steps. For IPSC experiments, a modified intracellular solution was used with a high chloride concentration (70 mM K-gluconate and 70 mM KCl) to augment γ-aminobutyric acid (GABA)ergic currents (reversal potential for chloride is ~−16 mV, hence, GABAergic currents are detected as inward currents). All IPSC experiments were done in the presence of 6,7-dinitroquinoxaline-2,3-dione (DNQX) (10 μM).

Nicotinic receptor currents on interneurons and pyramidal neurons were tested by pressure ejection of acetylcholine (Sigma, 1 mM) for 100 ms using a Picospritzer III (General valve corporation, Fairfield, NJ) from a glass electrode with a tip opening of ~1 μm. The puffer pipette was located ~20 μm from the soma and placed along the axis of the apical dendrite either before or behind the soma. The presence of atropine (200 nM) prevented stimulation of muscarinic receptors, and during all experiments, DNQX (10 μM) and bicuculline (1 μM) were used to block synaptic transmission. For network experiments acetylcholine was bath applied.

Analysis and Statistics for Electrophysiological Experiments

Frequency and amplitude of PSCs were analyzed using MiniAnalysis (Synaptosoft, Inc.). Local pressure application experiments were analyzed using custom made software for Matlab (Mathworks). To test for frequency differences in PSCs we used a Student's *t*-test. To test for amplitude differences in PSCs, we used a Kolmogorov–Smirnov test. To test for effects of pharmacology or genotype effects on nAChR currents induced by puff application of ACh, a Student's *t*-test was used. To test for differences in ratios of nAChR-positive and -negative cells in different layers, we used a Chi-square test. Significant results were obtained with a P value < 0.05. P values between 0.05 and 0.01 are shown as <0.05. P values between 0.01 and 0.001 are shown as $P < 0.01$ and P values lower than 0.001 are shown as $P < 0.001$.

Two-Photon Calcium Imaging

Loading

Slices were made as described before but in an alternative slicing solution (27 mM $NaHCO_3$, 1.5 mM NaH_2PO_4, 222 mM sucrose, 2.6 mM KCl, 0.5 mM $CaCl_2$, and 3 mM $MgSO_4$). Hereafter, slices were incubated in regular ACSF at 35 °C for 20 min and in room temperature for another 40 min. For bulk loading, a modified protocol based on Trevelyan et al. (2006) was used. Briefly, slices were first preincubated at 37 °C for 5 min in 3 mL ACSF containing 8 μL Cremophor EL solution (0.5% Cremophor EL in dimethyl sulfoxide [DMSO]). After this, 1 μL Fura-2-AM solution (25 μg Fura-2-AM with 4.5 μL DMSO and 0.5 μL pluronic acid) was pipetted on top of each slice. Then, the slices were left for incubation for 35–40 min after which they were put back in the slice chamber with ACSF at room temperature for at least 45 min.

Imaging

Experiments were performed in ACSF (perfusion speed 2.5 mL/min), continuously bubbled with 95% O_2/5% CO_2, at 32 °C. Imaging was performed using a multibeam 2-photon laser scanning microscope system (Trimscope, Lavision BioTec) coupled to a Ti:Sapphire laser (Chameleon, Coherent, excitation at 820 nm) and a CCD camera (C9100 Hamamatsu). The objective used had a 20× magnification and a 0.95 numerical aperture. The imaged plane was always in the same orientation with respect to the pia and the distance between them was determined for later analysis. The imaged area was 300 × 300 μm (pixel size of 0.6 μm, binning 2 × 2) and the imaging frequency was 9 Hz.

Experimental Protocol

Imaging was done during a 4-min baseline period, 2 min of ACh application, and a period of 8 min while washing out the applied drugs.

Analysis

Analysis was done using custom made software for Matlab (Mathworks). This program detected cell contours, extracted the fluorescence within these contours as a function of time, and detected events, after which manual inspection was done in a blind fashion. Cells were divided in 3 depth groups, corresponding to the measured thicknesses of the 3 layers in the PFC. Neurons that were between 100 and 300 μm, between 300 and 550 μm, and between 550 and 800 μm were considered to be part of, respectively, layers II/III, V, and VI.

For determining the activity in the different drug conditions, the percentage of neurons showing at least one calcium event was calculated per slice per minute. If slices included multiple layers, then, the slice was split up into 2 new slices containing just one layer. Effects of drugs, layer, and condition were tested using repeated measures analysis of variance (ANOVA), which were, if significant, followed by Newman–Keuls post hoc tests.

After this, for direct comparison of the activations in the different conditions, it was determined per neuron whether the activity after ACh application was higher, lower, or equal to the amount of calcium events in the minute before ACh application. Chi-square tests were performed to test if this statistic was different for the multiple layers, condition, and neuron types. In addition, binomial tests were used to determine the significance of the activation for every combination.

Determination of Cell Identity

High-resolution *z*-stacks were made to optimize the possibilities for identification (voxel size: 0.4 × 0.4 × 0.5 μm). For the majority of neurons, proximal dendrites showed strong fluorescence.

Cells were only taken into account if dendritic fluorescence was sufficient and cells could be identified as interneurons or pyramidal neurons according to the following criteria: 1) the presence of a clear apical dendrite, 2) a pyramidal shaped cell body for pyramidal neurons, 3) a clear nonpyramidal cell body morphology, and 4) bipolar or multipolar dendrite morphologies for the interneurons. Criteria 1 and 2 classified the neuron as pyramidal. Criteria 3 and 4 classified a neuron as interneuron. If the dendrites were not visible in the *z*-stack, the neurons were not categorized.

The identification of cells was done in a blind manner, that is, the experimenter was unaware of whether neurons were activated by nicotine receptor stimulation or not, excluding the possibility of a bias. After morphological identification, data were compared with electrophysiological experiments.

If neurons could not be unequivocally identified, they were excluded from statistics on cell type specific activation.

Histological Staining

For Nissl staining, 5 mice (P14–P19) were perfused with 0.9% NaCl, followed by 4% paraformaldehyde (PFA). After overnight fixation (4% PFA), slices of 100 μM were cut in sodium acetate using a vibratome. Slices were then photographed, to determine their size and to correct for shrinkage due to Nissl staining. Slices were then washed in sodium acetate buffer (4×, 10 min) and made permeable by sodium acetate + 0.5% Triton X (2 h). As a final step, they were stained with 0.5% cresyl violet (10–15 min). Layer borders were determined by cytoarchitectonic criteria (Van De Werd et al. 2010). Shown are the average layer depths of 9 slices along the rostral–caudal axis for all the animals. For identification of neuronal identity by morphology biocytin labeled neurons were revealed with chromogen 3,3′-diaminobenzidine tetrahydrochloride (DAB) using the avidin–biotin–peroxidase method and reconstructed using Neurolucida (Microbrightfield, USA) using a ×100 oil objective.

Results

nAChR Modulation of PFC Pyramidal Neurons

Pyramidal neurons in layer VI of the PFC are modulated by α5-containing β2* nAChRs (Kassam et al. 2008). Layer V pyramidal neurons showed no response to local application of high doses of nicotine (10 μM) (Couey et al. 2007). Whether layer II/III pyramidal neurons in the PFC are modulated by nAChRs is not

known. Therefore, we tested whether PFC pyramidal neurons show inward currents upon direct ACh application. We made whole-cell recordings from PFC pyramidal neurons in the different layers (Fig. 1) and used wild-type (WT), β2-null, or α7-null mice as well as pharmacological tools to determine the nAChR subunits involved. Pyramidal neurons were identified by their morphological appearance and based on the spiking profile in response to step depolarizations (Fig. 1*A1*). During recordings, neurons were filled with biocytin for post hoc identification by cell morphology (Figs 1*A1* and 2*A1*,*C1*). All recordings were done in the presence of 200 nM atropine to block muscarinic receptors as well as DNQX (10 μM) and bicuculline (1 μM) to block synaptic transmission. Local pressure application of ACh (1 mM, 100 ms) onto the soma of LII/III pyramidal cells showed that only a very small fraction of cells (3 of 24 neurons, 12.5%) displayed an inward current (Fig. 1*A2*–*A4*; amplitude 29.6 ± 8.0 pA). These findings show that only a minority of layer II/III pyramidal neurons are modulated by nAChRs. The inward currents showed the rapid activation and desensitization kinetics characteristic of α7 nAChRs (McGehee and Role 1995).

Next, we targeted layer V pyramidal neurons. In contrast to application of 10 μM nicotine (Couey et al. 2007), the majority of layer V pyramidal cells (27/31, 87%) displayed a rapid inward current upon ACh application (73.4 ± 13.0 pA, $n = 27$; Fig. 1*A2*–*A4*). The currents were reversibly blocked by the α7 nAChR antagonist methyllycaconitine (MLA; 71.0 ± 14.8 pA vs. −0.8 ± 0.9 pA [$n = 7$], $P < 0.01$). In addition, PFC layer V pyramidal neurons of transgenic mice lacking the α7 subunit showed no fast inward current (−0.4 ± 0.6 pA [$n = 8$], $P < 0.001$). These data suggest that the majority of layer V pyramidal neurons contain functional α7 nAChRs.

In line with previous reports (Kassam et al. 2008), we found that layer VI pyramidal neurons all showed slow inward currents (61.0 ± 9.6 pA, $n = 17$; Fig. 1*A2*–*A4*). The slow ACh-activated inward current was blocked by the antagonist of β2-containing nAChRs dihydro-β-erythroidine (DHβE, 74.5 ± 18.5 pA vs. 12.3 ± 3.8 pA [$n = 8$], $P < 0.01$) and was absent in transgenic mice lacking β2 subunits (3.0 ± 0.7 pA [$n = 7$], $P < 0.001$). However, in contrast to earlier reports, we did find that a subset of layer VI pyramidal cells showed an additional α7-like current (5/25, 20%; Supplementary Fig. S2). Taken together, these data show that a distinct modulation of pyramidal neurons by nAChRs exists in different prefrontal cortical layers. The majority of pyramidal neurons in layer II/III do not contain nAChRs. Pyramidal neurons in layer V are modulated by nAChRs containing α7 subunits, whereas pyramidal neurons in layer VI are under regulation of nAChRs containing β2 subunits, which are occasionally accompanied by α7-like currents (summarized in Fig. 8).

nAChR Modulation of Excitatory Synaptic Transmission in PFC Layers

In addition to direct depolarization by postsynaptic nAChRs on pyramidal neurons, nAChRs located on presynaptic glutamatergic inputs can augment the activity of pyramidal neurons by increasing glutamatergic signaling (McGehee and Role 1995; Mansvelder and McGehee 2000). Excitatory inputs to PFC layer V neurons were strongly augmented by activation of nAChRs containing β2 subunits ($n = 4$; Supplementary Fig. S2; Lambe et al. 2003; Couey et al. 2007). This augmentation was blocked by tetrodotoxin (TTX; 92.7 ± 18.9% of control, $n = 4$, $P < 0.01$; Supplementary Fig. S2), indicating that nAChRs are located on axonal compartments away from the presynaptic terminal. We investigated whether similar mechanisms exist in pyramidal neurons in other cortical layers by making simultaneous recordings of multiple pyramidal neurons in different layers and monitoring spontaneous excitatory transmission (Fig. 2), which was sensitive to DNQX (10 μM; Supplementary Fig. S2). In stark contrast to the frequency increase of EPSCs found in all layer V pyramidal neurons (991.6 ± 172% of control, $n = 21$, $P < 0.01$; Fig. 2*A3*,*C3*,*E1*), the frequency of EPSCs received by the

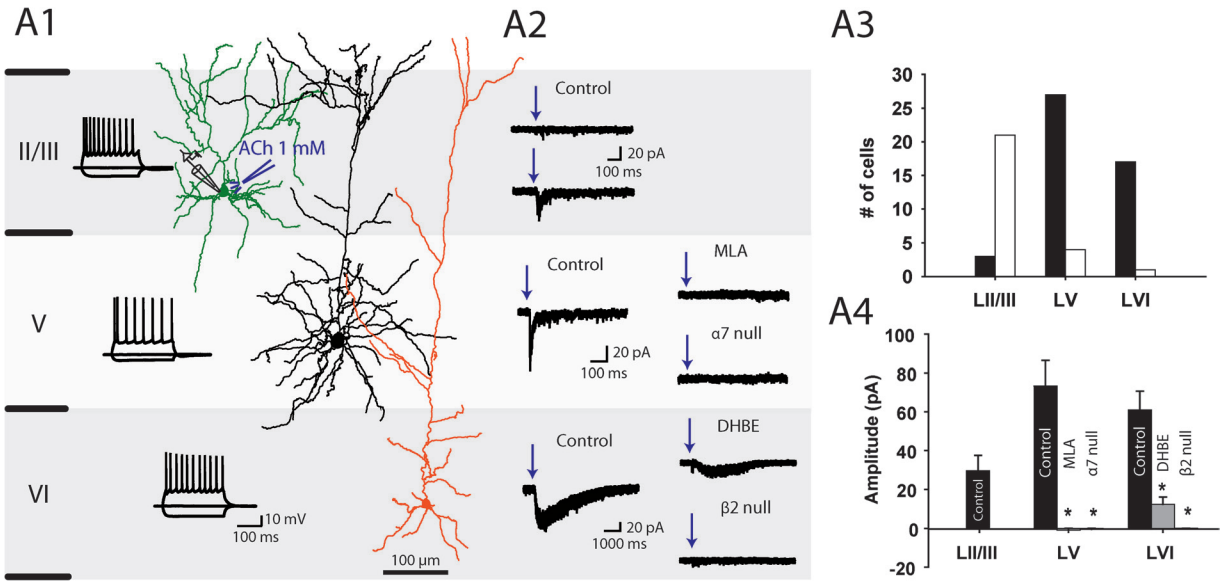

Figure 1. nAChR modulation of pyramidal neurons. (*A1*) Membrane potential responses to step current injections of pyramidal cells in the different layers of the medial PFC (current injections of −100 and +140 pA) and examples of post hoc reconstructed pyramidal neuron morphologies. (*A2*) Current responses of pyramidal neurons to local ACh (1 mM) application (all experiments in the presence of atropine 200 nM). Pyramidal neurons display a layer-specific modulation by nAChRs. (*A3*) Histogram quantifying the amount of pyramidal neurons positive (black) or negative (white) for functional nAChRs in each layer. (*A4*) Summary plot of average amplitudes of the ACh-induced currents. Currents in layer V pyramidal neurons were blocked by the α7 antagonist MLA ($n = 7$, Student's *t*-test, $P < 0.01$) and absent in mice lacking the gene for the α7 subunit ($n = 8$, Student's *t*-test, $P < 0.001$). Currents in layer VI pyramidal neurons were blocked by β2* antagonist DHβE ($n = 8$, Student's *t*-test, $P < 0.01$) and absent in β2-null mice ($n = 7$, Student's *t*-test, $P < 0.001$).

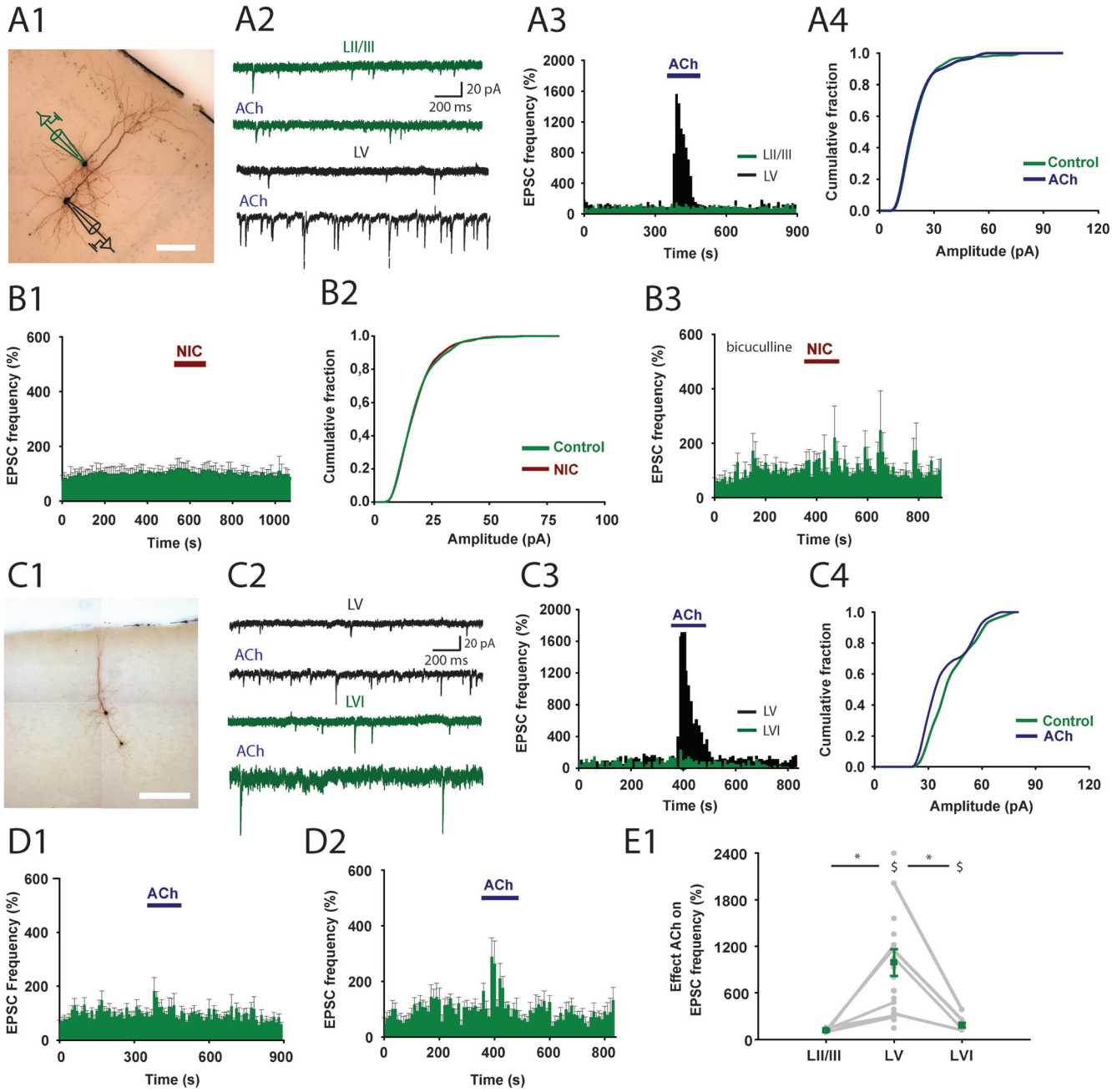

Figure 2. nAChR modulation of glutamatergic synaptic transmission. (*A1*) Biocytin-filled cells showing the morphology of 2 pyramidal neurons in layers II/III and V recorded simultaneously. On top, the recording setup for data in *A2–A4* is depicted. Scale bar = 100 μm. (*A2*) Example traces of spontaneous excitatory transmission (EPSCs) during baseline (top) and ACh (1 mM) application (bottom) for a double recording of LII/III (green) and LV (black). (*A3*) Histogram of the EPSC frequency. Same neurons as in A2. (*A4*) Cumulative amplitude distribution of EPSCs recorded from a layer II/III pyramidal neuron. ACh application had no effect on the distribution (Kolmogorov–Smirnov test, $P > 0.05$). (*B1*) Histogram showing the average EPSC frequency over time during nicotine (10 μM) application ($n = 11$). (*B2*) Cumulative amplitude distribution of EPSCs recorded from a layer II/III pyramidal neuron. Nicotine (10 μM) application had no effect on the distribution ($n = 11$, Kolmogorov–Smirnov test, $P > 0.05$). (*B3*) Same experiment as in *B1* in addition of the GABAa receptor blocker bicuculline (10 μM). (*C1–C3*) Same as in *A1–A3* but now for a layer V (black) and LVI pyramidal neuron (green). Scale bar = 250 μm. (*C4*) Cumulative amplitude distribution of EPSCs recorded from a layer VI pyramidal neuron. ACh application had no effect on the distribution (Kolmogorov–Smirnov test, $P > 0.05$). (*D1*) Average EPSC frequency histogram of layer II/III pyramidal neurons ($n = 8$). Duration of ACh application is indicated by blue bar. (*D2*) Average EPSC frequency histogram of layer VI pyramidal neurons ($n = 8$). Duration of ACh application is indicated by blue bar. (*E1*) Summary plot of ACh effects on EPSC frequency in pyramidal neurons from different layers. Individual recordings are shown with grey dots. Simultaneous recordings in different layers are connected with grey line ($n = 6$ layer II/III and LV, $n = 4$ layer V and LVI). Green dot shows average frequency during acetylcholine application. Layers V and VI showed a significant increase in EPSC frequency on ACh application (Indicated by $, $n = 21$, Student's *t*-test, $P < 0.01$ and $n = 8$, Student's *t*-test, $P = 0.03$). The increase in EPSC frequency was significantly lower in LVI (Student's *t*-test, $P < 0.01$). All error bars in figure indicate standard error of the mean.

simultaneously recorded layer II/III pyramidal neurons showed no change (112.8 ± 8.4%, $n = 8$, $P = 0.08$; Fig. 2*A2*,*A3*,*D*,*E*). The amplitude distribution of the EPSCs in layer II/III pyramidal neurons did not change in the presence of ACh ($n = 8$, $P > 0.05$ for all cells; Fig. 2*A4*) also in contrast to the increase in amplitude by ACh application found in all layer V pyramidal neurons ($n = 20/21$, $P < 0.05$, data not shown). Similar to ACh, application of nicotine (10 μM) did not alter the frequency and

amplitude of EPSCs in layer II/III pyramidal neurons (106.7 ± 4.2%, $n = 10$, $P = 0.34$; Fig. 2*B1*). To test whether a potential effect of nAChR activation on excitatory transmission could be masked by a simultaneous effect of ACh on inhibition (Couey et al. 2007), bicuculline (10 μM) was applied to block inhibitory transmission. No effect was found of nAChR stimulation on the frequency of EPSCs received by layer II/III pyramidal neurons (127.3 ± 9.5%, $n = 4$, $P = 0.06$; Fig. 2*B3*). These findings show that ACh does not modify excitatory synaptic transmission received by layer II/III pyramidal neurons, which suggests that glutamatergic inputs to these neurons do not contain functional nAChRs.

Simultaneous recordings of layer V and VI pyramidal neurons showed that layer VI pyramidal neurons experienced a significantly smaller increase in EPSC frequency by ACh application than layer V pyramidal neurons ($P < 0.01$). Only a transient small increase was detected (185.1 ± 32.0%, $n = 8$, $P = 0.03$; Fig. 2*C2,C3,D,E*). An increase in amplitude was detected in only 1 of 8 cells (Fig. 2*C4*). These data show that excitatory inputs to layer VI pyramidal neurons are mildly modulated by ACh through nAChR activation. In conclusion, in contrast to layer II/III pyramidal neurons, both layer V and layer VI pyramidal neurons experience increased frequencies of excitatory inputs in the presence of ACh (summarized in Fig. 8).

Modulation of Inhibitory Inputs to Pyramidal Neurons by nAChRs Is Limited to Layers II/III and V

Besides pyramidal neurons, also interneurons are modulated by nAChRs. In layer V, nAChRs are expressed by different types of interneurons (Couey et al. 2007). Activation of nAChRs on interneurons increases action potential firing and augments the frequency of GABAergic inputs to pyramidal neurons (Alkondon et al. 2000; Ji and Dani 2000; Couey et al. 2007). It is not known whether interneurons in other medial PFC layers contain functional nAChRs. It is also not known whether pyramidal neurons in layers II/III and VI of the PFC experience increased inhibition when nAChRs are activated. We hypothesized that interneurons in cortical layers II/III and VI are also modulated by nAChRs. To test this, we made simultaneous whole-cell recordings of pyramidal neurons in different layers and monitored IPSCs upon ACh application (Fig. 3*A*). All currents could be blocked by the GABAa receptor antagonist bicuculline (10 μM, $n = 5$; Supplementary Fig. S3). In layer II/III pyramidal neurons, application of ACh increased the frequency of IPSCs ($P < 0.05$ for 8 of 10 neurons; Fig. 3*A,B,D*). In simultaneously recorded layer V pyramidal neurons, a similar increase in IPSC frequency upon ACh application was found in 15 of 16 cells ($P < 0.05$; Fig. 3*A,B,D*). Between layer II/III and layer V pyramidal neurons, no significant difference in frequency increase was observed ($P = 0.5$; Fig. 3*D*). In both layers, the amplitude of IPSCs showed a shift toward larger amplitudes in the majority of pyramidal cells (6 of 10 layer II/III neurons, 10 of 16 layer V neurons, $P < 0.05$; Fig. 3*C*). In both layer V and layer II/III pyramidal neurons, the effects on frequency and amplitude of IPSCs were blocked by the antagonist for nAChRs mecamylamine (LII/III: 505.3 ± 148.2% of control [$n = 10$] vs. 117.9 ± 9.2% [$n = 3$], $P < 0.05$. LV: 351.2 ± 42.8% [$n = 16$] vs. 87.4 ± 3.4% [$n = 3$], $P < 0.01$; Fig. 3*E* and Supplementary Fig. S2) and sodium channel blocker TTX (LII/III: 505.3 ± 148.2% [$n = 10$] vs. 101.3 ± 13.8% [$n = 2$], $P < 0.05$. LV: 351.2 ± 42.8% [$n = 16$] vs. 108.6 ± 8.2% [$n = 3$], $P < 0.01$; Fig. 3*E* and Supplementary Fig. S2). This suggests that these nAChR effects are not mediated by presynaptic receptors but by receptors located on perisomatic compartments of interneurons. In contrast, the majority of layer VI pyramidal neurons showed no changes in IPSC frequency or amplitude in response to ACh application (10 of 12 cells showed no response, $P > 0.05$; Fig. 3*A–D*). In 2 of 12 pyramidal neurons, ACh did increase IPSC frequency and amplitude (not shown). Taken together, these data suggest that in layers II/III and V, inhibitory synaptic transmission received by pyramidal neurons is augmented by nAChR stimulation, whereas in layer VI, inhibitory inputs to the majority of pyramidal neurons are not controlled by nAChRs.

nAChR Modulation of PFC Nonfast-Spiking Interneurons

Different types of interneurons in PFC layer V express various types of nAChRs (Couey et al. 2007). Which interneurons in layers II/III and VI contain nAChRs is not known. Using WT, β2-null, and α7-null mice as well as pharmacology in whole-cell recordings from interneurons, we tested which interneuron subtypes are modulated by nAChRs. We distinguished between 2 types of inhibitory neurons: fast-spiking (FS) interneurons and nonfast-spiking (NFS) interneurons (Kawaguchi and Kubota 1997), which can be distinguished based on morphology and action potential firing characteristics (Figs 4*A1,A2* and 5*A1,A2* and Supplementary Table 1). FS interneurons showed high action potential firing frequency and had a low input resistance (183.0 MΩ ± 13) and narrow spike width (0.49 ms ± 0.02, $n = 32$; Supplementary Table 1 and Fig. 5). NFS cells showed a broader spike width (0.96 ms ± 0.03, $P < 0.05$) and a higher input resistance (331 MΩ ± 13, $P < 0.05$, $n = 76$; Supplementary Table 1 and Fig. S4). Upon direct application of ACh (in the presence of atropine, 200 nM, and DNQX, 10 μM, and bicuculline, 1 μM) NFS cells in layers II/III and V showed mixed responses (Fig. 4*A3*). In layer II/III, 29 of 47 cells showed a response to ACh (Fig. 4*B1*). In 9 of these 29 NFS neurons, a slow current was activated that was most likely mediated solely by nAChRs containing the β2 subunit (Figs 4*A3* and 5*B1,B2*), since slow currents were blocked by DHβE and absent in β2-null mice (Fig. 4*A5*). Seven of 29 NFS cells showed only a rapid α7-like inward current. Rapid inward currents that were present in β2-null mice were blocked by MLA ($n = 5$, $P < 0.01$; Supplementary Fig. S2) and absent in α7-null mice (Fig. 4*A3–A5,B1,B2*). Close to half of the NFS cells in which ACh induced an inward current, a mixed current was detected that was most likely mediated by both β2* and α7 nAChRs (Fig. 4*A3,B1*). MLA blocked the fast component of this current, whereas DHβE blocked the slow component ($n = 2$; Fig. 4*A4*). Within the group of NFS neurons, a subpopulation of neurons expresses somatostatin. These cells mainly target distal tufts of pyramidal cells (Kawaguchi and Kondo 2002; Silberberg and Markram 2007) and have been shown to express nAChRs in layer V (Couey et al. 2007). To test whether somatostatin-positive cells in LII/III also contain functional nAChRs, we used the GIN-line that expresses eGFP in somatostatin-positive cells in superficial layers (Ma et al. 2006). All somatostatin-positive cells tested showed inward currents upon ACh application. Most cells showed slow inward currents reminiscent of β2*-like nAChRs (4 of 5 cells, 80%), whereas one cell displayed the rapid α7-like nAChR response (Fig. 4*B3*).

In layer V, a larger proportion the NFS cells showed an inward current upon direct ACh application (85.7% vs. 68.4%,

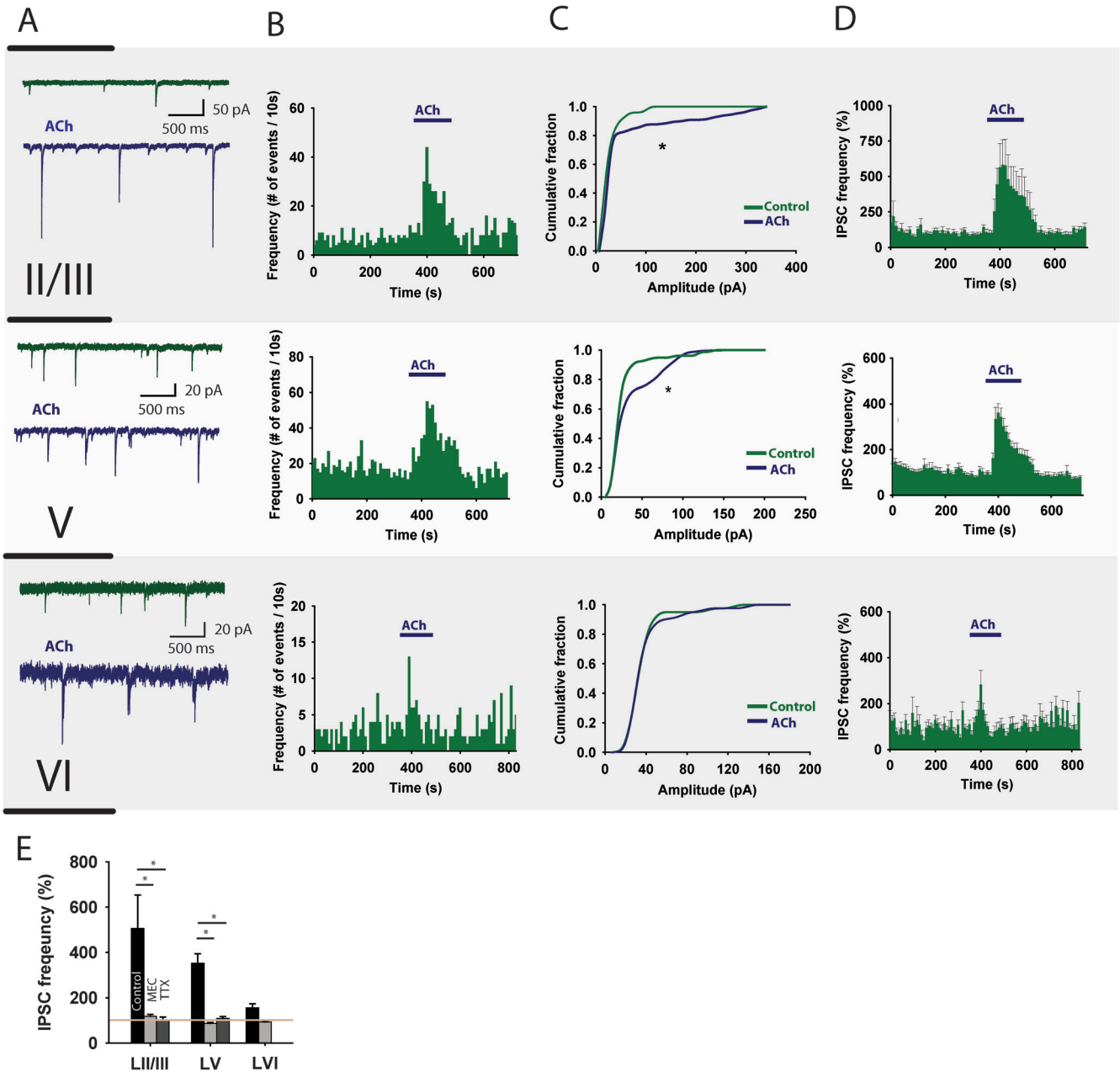

Figure 3. nAChR modulation of inhibitory transmission received by pyramidal neurons. (*A*) Example traces showing spontaneous IPSCs recorded from PFC pyramidal neurons in the absence (green) and presence of 1 mM ACh (blue). (*B*) Histograms showing the frequency of IPSCs during a single experiment. (*C*) Cumulative amplitude distribution showing that during acetylcholine application IPSCs with larger amplitude appeared in layers II/III (6 of 10 neurons) and LV (10 of 16 neurons, Kolmogorov–Smirnov test, $P < 0.05$) but not in layer VI (10 of 12 neurons, Kolmogorov–Smirnov test, $P > 0.05$). (*D*) Average IPSC frequency histogram for pyramidal neurons in different PFC layers during acetylcholine application. Blue bar indicates the time when acetylcholine is present. Acetylcholine significantly increased the IPSC frequency in LII/III (505.3 ± 148.2%, Student's t-test, $P < 0.01$) and LV (351.2 ± 42.8%, $P < 0.001$) but not in LVI (153.6 ± 18.4%, $P = 0.09$). (*E*) Summary bar graph quantifying the effect of acetylcholine and different blockers on the IPSC frequency measured in prefrontal cortical pyramidal neurons (mecamylamine; LII/III: 505.3 ± 148.2% of control [$n = 10$] vs. 117.9 ± 9.2% [$n = 3$], $P < 0.05$. LV: 351.2 ± 42.8% [$n = 16$] vs. 87.4 ± 3.4% [$n = 3$], $P < 0.01$, TTX; LII/III: 505.3 ± 148.2% [$n = 10$] vs. 101.3 ± 13.8% [$n = 2$], $P < 0.05$. LV: 351.2 ± 42.8% [$n = 16$] vs. 108.6 ± 8.2% [$n = 3$], $P < 0.01$).

$P < 0.001$; Fig. 4*B1*). ACh induced in 18 of 21 layer V NFS cells mixed inward currents (Fig. 4*A3*). As with layer II/III NFS cells, these fell into 3 groups: one group of NFS cells showed only β2-like nAChR-mediated slow currents (Fig. 4*A3*). A second group showed only fast α7-like inward currents, whereas the third group showed a mix of fast and slow currents (Fig. 4*A3*,*B1*,*B2*).

In layer VI, all 8 recorded NFS cells showed slow ACh-induced inward currents of 38.4 ± 8.4 pA (Fig. 4*A3*,*B1*,*B2*). Thus, nAChR modulation of NFS interneurons in PFC is layer specific, with a higher proportion of NFS cells in deep layers that contain functional nAChRs. β2-containing and α7 nAChRs are found separately or on the same neuron in layers II/III and V. Layer VI NFS neurons display currents reminiscent of β2-containing nAChRs (summarized in Fig. 8).

nAChR Modulation of Fast-Spiking Interneurons

In contrast to NFS cells, FS cells in all PFC layers did not show β2-containing nAChR-mediated inward currents upon ACh

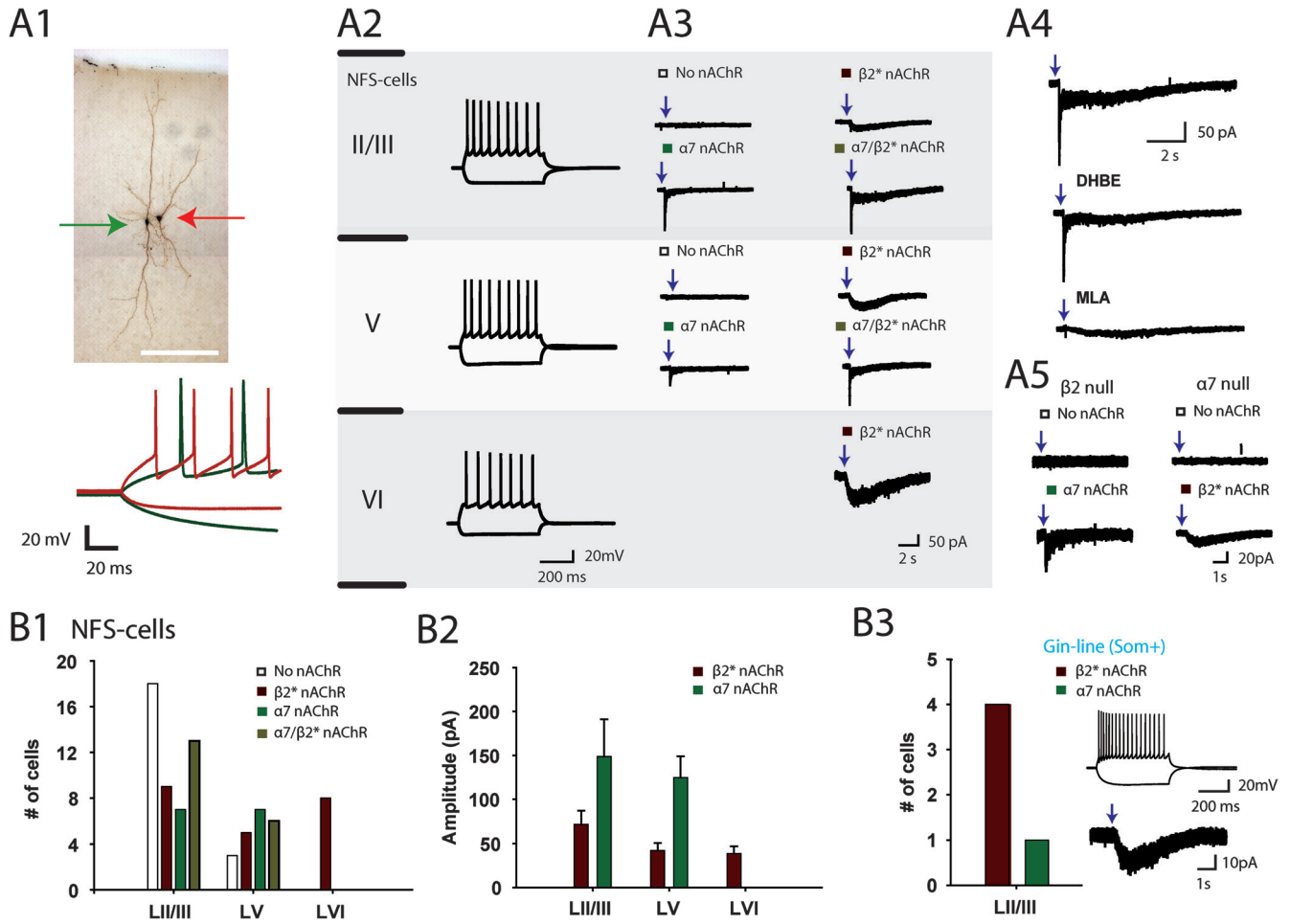

Figure 4. nAChR modulation of NFS interneurons. (*A1*) Biocytin staining of NFS and FS interneurons in layer V. Lower panel shows characteristic action potential firing of NFS and FS cells. Scale bar is 250 μM. (*A2*) Spike profile of NFS interneurons in different layers (current injection −100 and +140 pA). (*A3*) Example traces of ACh-induced responses in NFS interneurons. Fast α7-like, slow β2*-like, and mixed nAChR responses were observed. (*A4*) NFS cell showing mixed nAChR response. Fast α7-like components were blocked by MLA (10 nM), whereas the slow β2*-like component was blocked by DHβE (10 μM). (*A5*) Example traces of NFS cells recorded in β2- and α7-null mice. β2-null mice only exhibited fast onset nAChR responses or cells without a nAChR response. α7-null mice showed either no nAChR response or slow nAChR responses. (*B1*) Histogram summarizing the nicotinic receptor distribution on NFS cells for each layer. (*B2*) Average amplitude of the α7-like and β2*-like nAChR-mediated responses in different layers. (*B3*) Somatostatin-positive cells expressing eGFP are positive for β2*-like nAChR-mediated currents.

application. All inward currents recorded in FS cells had fast onset and decay kinetics, reminiscent of α7 nAChRs, and were 78.3 ± 20.7 pA (LII/III) and 64.9 ± 11.2 pA (LV) in amplitude (Fig. 5*A3*,*B1*,*B2*). Layer II/III contained the highest proportion of nAChR containing FS cells. Nine of 11 FS neurons showed the fast inward current that was blocked by MLA (n = 3, P = 0.04; Fig. 5*A3*,*B3*) and was absent in α7-null mice (n = 2, P < 0.01; Fig. 5*B3*). In layer V, 7 of 13 cells expressed fast ACh-induced inward currents (Fig. 5*B1*,*B2*). In layer VI, 6 FS cells were detected, and they did not contain nicotinic receptors. Taken together, the majority of FS cells in layer II/III and about half of the FS cells in layer V contain functional nAChRs of the α7 subtype (summarized in Fig. 8).

Network Modulation of the Prefrontal Cortex by nAChRs

Cholinergic signaling in the PFC can occur on a timescale of seconds to minutes (Parikh et al. 2007; Sarter et al. 2009). Our data show that nicotinic receptors are expressed by inhibitory neurons in layer II/III and by both excitatory and inhibitory neurons in layer V and layer VI. How activation of the nAChRs on these opposing types of neurons affects the balance of neuronal activity in the different layers when acetylcholine levels increase in the PFC is not known. In addition, layer V pyramidal neurons get activated through presynaptic β2* nAChRs, whereas layer VI pyramidal neurons are stimulated through postsynaptic β2* receptors directly. How activation of the receptors alters the balance of activity among these different layers is not known. Given the distribution of nAChRs across the layers, we hypothesize that activation of the PFC by nAChRs is layer specific. To test this, we monitored neuronal activation in different layers with single-cell resolution by 2-photon imaging of medial PFC slices that were bulk loaded with the calcium indicator Fura-2-AM (Fig. 6). Changes in fluorescence were proportional to the amount of action potential firing in activated neurons, as reported in the literature (Supplementary Fig. S1; Cossart et al. 2005). The depth of prefrontal cortical layers II/III, V, and VI was determined by post hoc Nissl staining (Fig. 6*C*,*D*). Subsequently, neurons were assigned to layers by their distance from the pia. After baseline activity was recorded in the presence of the muscarinic receptor blocker atropine (200 nM) for at least 4 min, acetylcholine (ACh, 1 mM) was applied for 2 min. During baseline, neuronal activity was low: every minute on average

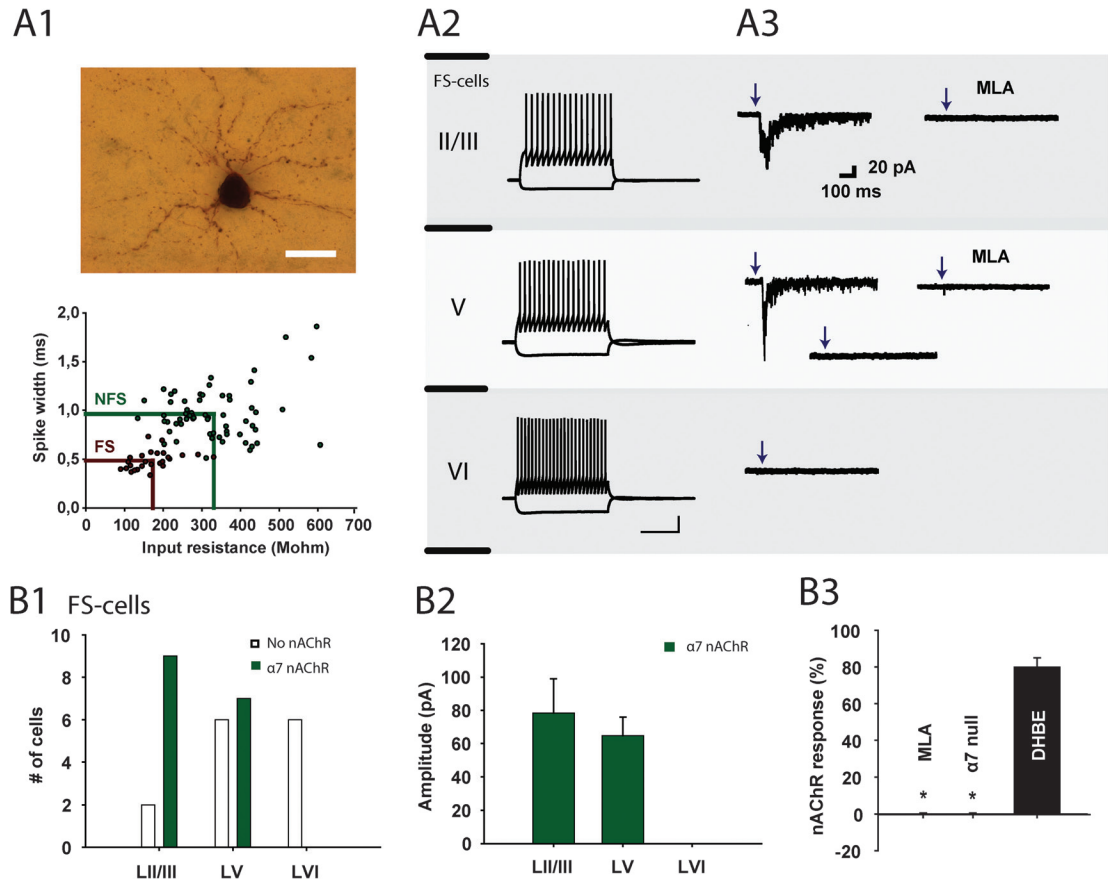

Figure 5. nAChR modulation of FS interneurons. (*A1*) Biocyting staining of an FS interneuron. Lower panel indicates spike width and input resistance for FS and NFS cells. Scale bar = 25 μm. (*A2*) Spike profile of FS interneurons in different layers. (*A3*) Example traces of ACh-induced responses in FS interneurons. α7-mediated responses were observed in layer II/III and half of the layer V neurons (positive and negative example shown) but not in layer VI. (*B1*) Histogram summarizing the amount of FS cells positive for nAChRs. (*B2*) Summary of the average amplitudes of α7 currents on FS cells per layer. (*B3*) All nAChR-induced currents on FS cells could be blocked by MLA ($n = 3$) but not by DHβE ($n = 2$). FS cells in α7-null mice were not found to express functional nAChRs ($n = 2$).

2.46% ± 0.35% of the neurons ($n = 82$ slices) exhibited at least one fluorescence transient (Fig. 6*A,B,E*). During wash in of ACh, a higher proportion of the cells in the slices displayed fluorescence transients (Fig. 6*A,B,E*). Increased activity was found across all layers (Fig. 6*E*). Neuronal activity in LVI (550–800 μm) was most strongly affected by nAChR stimulation (14.2 ± 3.1% active cells, $P < 0.001$). In contrast, in LII/III (100–300 μm), only moderate numbers of neurons were activated during nAChR stimulation (5.7 ± 1.8%, $P = 0.24$; Fig. 6*E*). Nicotinic AChR activation induced intermediate amounts of activity in LV (300–550 μm; 9.6 ± 1.3%, $P < 0.01$). Baseline activity was not significantly different between layers and wash out of ACh resulted in activity levels similar to baseline ($P = 0.87$, 0.97 and 0.64 for, respectively, LII/III, V, and VI). nAChR-induced activity was completely absent in the presence of the nAChR antagonist mecamylamine (10 μM, –0.3 ± 1.6% activation, $P = 0.85$).

The cell types that were activated by nAChR stimulation were identified from high-resolution *z*-stacks of the imaged slices (see Materials and Methods). More than half of the individual neurons could be identified as either pyramidal or interneuron based on morphology (Fig. 6*F*). We found that nAChR stimulation activated interneurons similarly across all layers (Fig. 6*G*). Layer II/III pyramidal neurons showed no change in activity upon nAChR stimulation ($P = 0.6$). This is in contrast to layer V and layer VI where, besides interneurons, also pyramidal neurons were prominently activated by nAChR stimulation ($P < 0.01$ and $P < 0.001$). The increase in pyramidal neuron activity was significantly different for the PFC layers ($P < 0.01$) (Fig. 6*G*). Taken together, nAChR stimulation results in more neuronal activity in LV and LVI of the PFC activating both pyramidal and interneurons. In superficial layers, fewer cells show activity upon nAChR stimulation, and these are all interneurons.

Neuronal Network Activation by nAChRs Is Mediated by β2 nAChRs*

Our results show that neurons in the PFC can be stimulated through both α7 and β2-containing nAChRs. Modulation of layer VI neurons is dominated by β2* nAChRs. However, LV pyramidal neurons are stimulated through presynaptic β2* nAChRs and postsynaptic α7 nAChRs. Also interneurons in LII/III and LV show mixed β2* and α7 responses. To investigate the contribution of α7 and β2* nAChR in inducing network activity during ACh concentration changes at the scale of seconds to minutes, we imaged neuronal activity upon ACh bath application in β2- and α7-null mice (Fig. 7). Both WT and α7-null mice show strong layer-dependent activations (Fig. 7*A–C* [WT: $P < 0.001$; α7 null: $P < 0.001$]: WT layer II/III: $P < 0.01$; layer V: $P < 0.001$; layer VI: $P < 0.001$; α7 null: layer II/III: not significant, ns; layer V: $P < 0.001$; layer VI: $P < 0.001$), whereas none of the layers showed a significant activation in β2-null mice (Fig. 7*A–C*). The activation

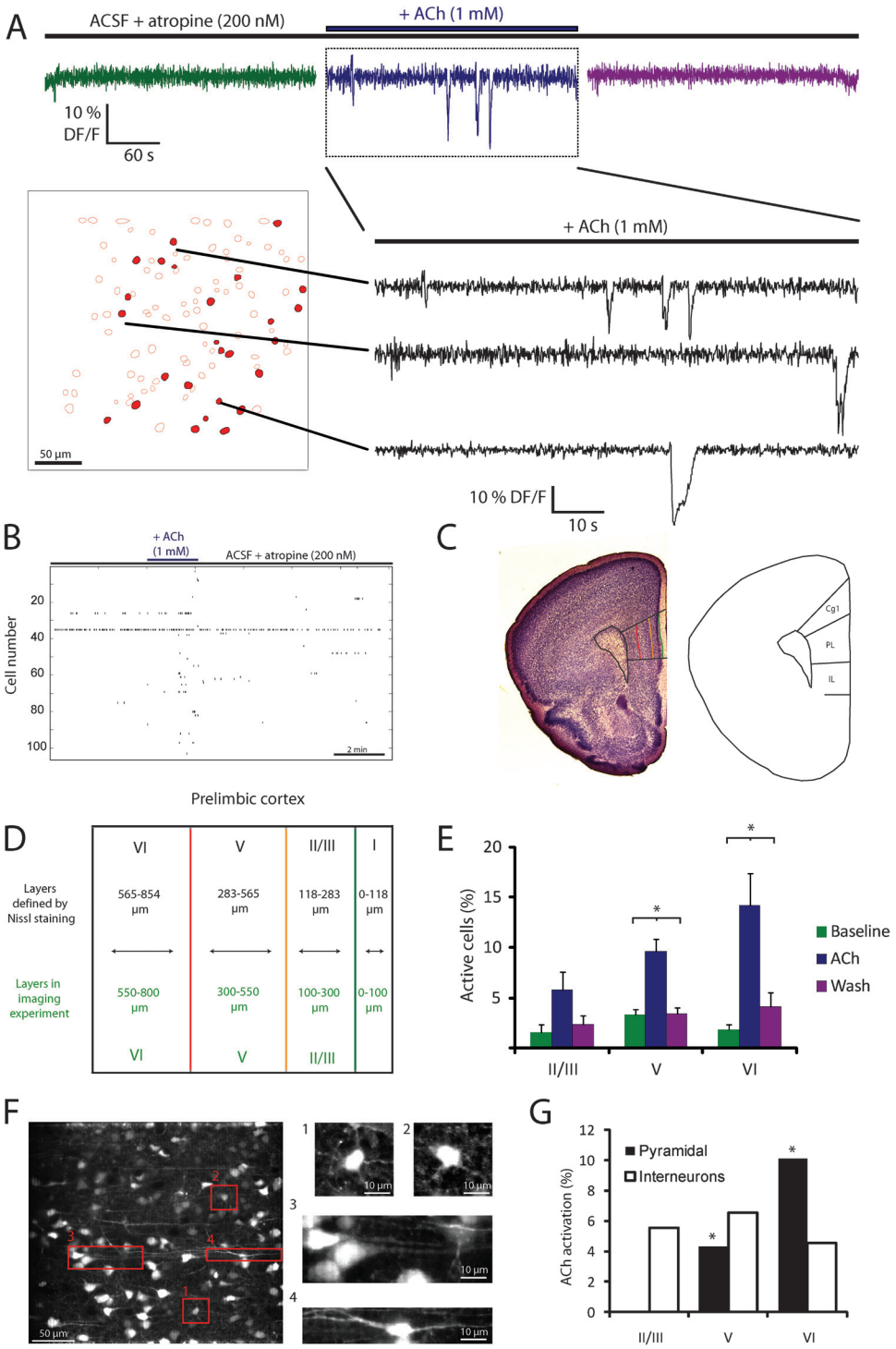

Figure 6. ACh-induced neuronal activation is most prominent in deep layers. (*A*) Top traces: schematic representation of the experimental protocol and an example of the fluorescence of one cell during the entire experiment. Bottom panels: example of automatically detected cell contours and fluorescence traces from these cells. Cells that are indicated in red showed increased activity during ACh application. Fluorescence traces of 3 highlighted neurons during ACh application show downward deflections that indicate calcium influx due to neuronal activity. (*B*) Rasterplot of network activity during a single experiment. Black ticks represent the occurrence of a calcium event. During application of ACh, there is an increase in the number of cells showing calcium events. (*C*) Left: example of a Nissl-stained coronal slice, prelimbic area is indicated by black lines. Colored lines indicate the depth of layers within the prelimbic area (yellow is LII/III, red is LV, and LVI is black). Right: schematic cartoon indicating the medial prefrontal cortical areas. (*D*) Overview of the average depth of prefrontal cortical layers defined by Nissl staining (upper black values) and depth of layers used to categorize the imaged cells (lower green values). (*E*) Percentage of cells that is active per minute in different layers ($n = 82$ slices). ANOVA repeated measure testing indicated that the drug effect ($P < 0.001$) and its interaction with the layers ($P < 0.05$) are significant. In deep layers, there is a significant effect of ACh application (layer V: $P < 0.01$ [$n = 37$]; layer VI: $P < 0.001$ [$n = 23$, Newman–Keuls post hoc test]). During wash out, activity returned to baseline (layer V: $P < 0.01$; layer VI: $P < 0.001$). (*F*) Example of identification of neurons. On the left, a collapsed *z*-stack at high resolution. On the right, examples of identified neurons, interneurons (1, 2, and 4), and pyramidal neurons (3). (*G*) Percentage of identified pyramidal and interneurons which activity was increased during ACh application. Pyramidal cells showed a significant increase in the percentage of cells that was active in both layer V ($P < 0.01$) and layer VI ($P < 0.001$, binomial test). In addition, the size of the activation was significantly different between layers ($P < 0.01$). Interneuron activation was not significantly different between the 3 layers. All error bars represent standard error of the mean.

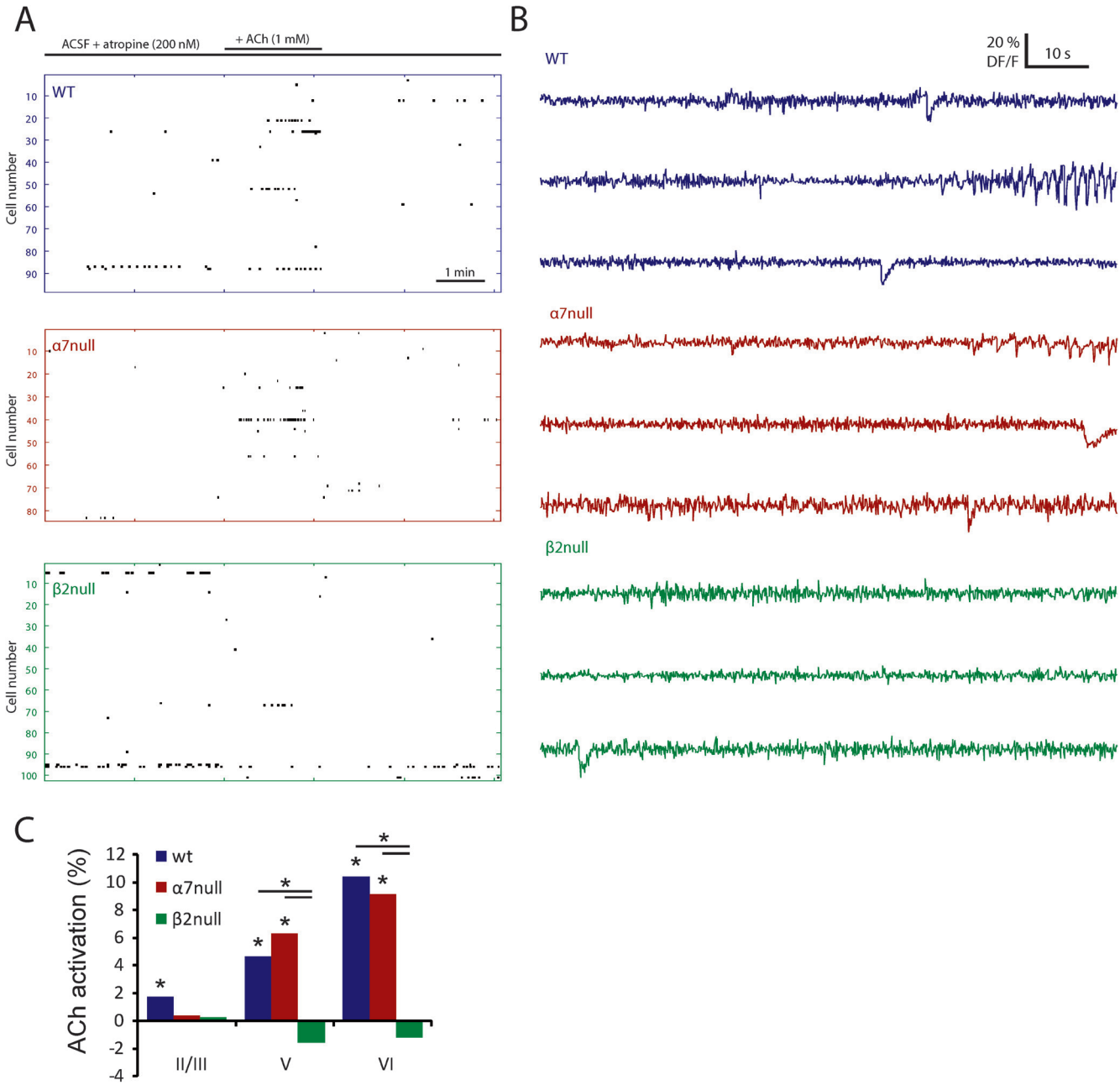

Figure 7. ACh-induced network activity in α7- and β2-null mice. Activation of PFC neurons by ACh (1 mM) in mice lacking β2 and α7 subunits shows a strong contribution of β2 subunits to the observed activation of the network. (*A*) Rasterplot of network activity in slices from WT, α7-null and β2-null mice. (*B*) Fluorescence traces during ACh application for WT, α7-null and β2-null mice. (*C*) Summary histogram showing that both WT and α7-null mice show strong layer-dependent (WT: $P < 0.001$; α7 null: $P < 0.001$) activations (binomial tests: WT layer II/III: $P < 0.01$; layer V: $P < 0.001$; layer VI: $P < 0.001$; α7 null: layer II/III: not significant, ns; layer V: $P < 0.001$; layer VI: $P < 0.001$), whereas none of the layers shows a significant activation in β2-null mice. The activation is significantly stronger in PFC slices of WT and α7-null than in β2-null animals in layer V and layer VI (WT vs. β2 null: layer V: $P < 0.001$; layer VI: $P < 0.001$; α7 null vs. β2 null: layer V: $P < 0.001$; layer VI: $P < 0.001$).

was significantly stronger in PFC slices of WT and α7-null than in β2-null animals in layer V and layer VI (WT vs. β2 null: layer V: $P < 0.001$; layer VI: $P < 0.001$; α7 null vs. β2 null: layer V: $P < 0.001$; layer VI: $P < 0.001$). Hence, although layer V neurons show prominent expression of α7 nAChRs on pyramidal and interneurons, no change in activity was found. Only in LII/III, we did not find a significant activation upon application of ACh in α7-null mice, but activity levels were not statistically different from WT.

Thus, nAChR-induced neuronal activation across PFC layers strongly depends on β2-containing nAChRs when ACh levels rise in a sustained manner on a timescale of seconds to minutes. These data may suggest that the relatively slow changes in ACh concentrations do not result in strong enough inward currents mediated by α7 nAChRs to induce action potential firing by neurons. To test this, we recorded from layer V pyramidal neurons and compared the peak amplitude of α7 currents induced by puff application and bath application on the same cells. Peak amplitude was high during puff application, while bath application resulted in low amplitude currents (Supplementary Fig. S4). This is in contrast to β2* nAChRs on

layer VI pyramidal neurons which reached similar peak amplitudes during both types of ACh application. These data suggest that when ACh levels rise in the PFC on the scale of seconds to minutes (Sarter et al. 2009), neuronal activation is predominantly mediated by β2-containing nAChRs.

Discussion

Activation of the PFC by nAChRs will depend on which cell types express nAChRs and what subunits they are made of. Since nAChRs modulate excitatory as well as inhibitory neurons in the PFC circuitry, an understanding of how the PFC output is affected by nAChR activation requires an integrated view of nAChR-induced activity in the PFC. Using a combined approach of whole-cell recordings and 2-photon network imaging, we find in this study that 1) PFC pyramidal neurons in different layers show a differential pattern of nAChR modulation: layer II/III pyramidal neurons do not contain nAChRs, layer V pyramidal neurons contain α7 nAChRs, and layer VI pyramidal neurons are modulated by β2* nicotinic receptors; 2) glutamatergic inputs to layer II/III are not regulated by nAChRs in contrast to excitatory inputs to layer V and layer VI pyramidal neurons; 3) interneurons show differential patterns of nAChR modulation, in layers II/III and V, α7 and β2* nAChRs are found, whereas in layer VI, only β2* nAChRs are found (summarized in Fig. 8); 4) nAChRs stimulate both excitatory and inhibitory neurons in layers V and VI, and this results in a net augmentation of activity of layer V and VI pyramidal neurons, whereas in layer II/III, only interneurons are activated; and 5) network activity in the PFC in response to bath application of ACh is layer specific and dominated by β2* nAChRs.

Layer-Specific nAChR Modulation of PFC Pyramidal Neurons

In the PFC, nAChR expression is found across all layers (Gioanni et al. 1999). nAChRs can alter pyramidal neuron activity by enhancing glutamatergic inputs or by activating postsynaptic receptors directly (Poorthuis et al. 2009). Hippocampal pyramidal neurons express functional α7 nAChR (Ji et al. 2001). In motor cortex, somatosensory cortex, and visual cortex, layer II/III and layer V pyramidal neurons do not contain nAChRs (Nicoll et al. 1996; Gil et al. 1997; Xiang et al. 1998; Porter et al. 1999; Gulledge et al. 2007). We find that PFC layer II/III pyramidal cells also do not contain nAChRs and also glutamatergic inputs to these pyramidal neurons are not modulated by nAChRs. Hence, nAChRs do not augment the output of superficial pyramidal neurons.

In contrast, in layer V pyramidal neurons, activation of presynaptic β2* nAChRs on glutamatergic inputs from the thalamus strongly enhances activity of these neurons (Gioanni et al. 1999; Lambe et al. 2003; Couey et al. 2007). We find that these presynaptic mechanisms are specific to layer V, as they are absent in layers II/III and VI. This may suggest that nAChR-mediated modulation of thalamic inputs to the PFC is

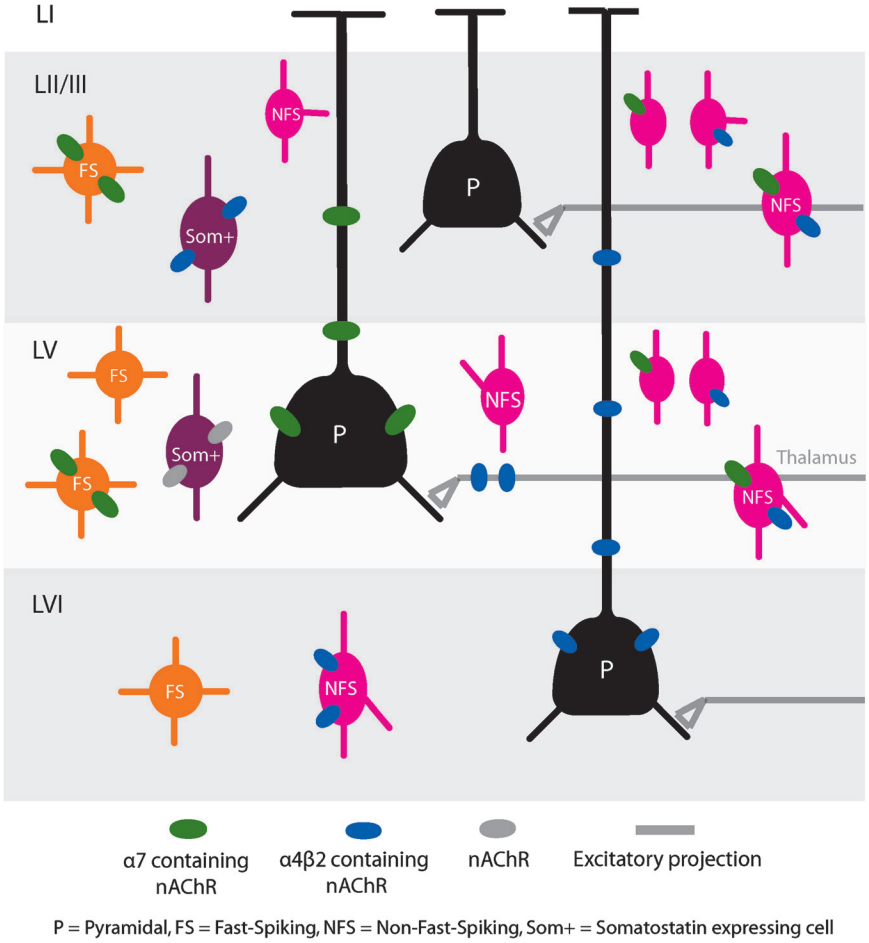

Figure 8. Overview of nicotinic receptor modulation of the different cell types in all PFC layers.

specifically targeting layer V pyramidal neurons, which project-mainly to the striatum and hypothalamus (Gabbott et al. 2005). Nicotinic enhancement of thalamic inputs to the cortex also plays a role in primary sensory areas, where it enhances sensory representation in the cortical target structure (Penschuck et al. 2002; Disney et al. 2007; Kawai et al. 2007). In addition to presynaptic β2* nAChRs that can augment its activity, layer V pyramidal neurons also contain postsynaptic α7 nAChRs. In contrast to layer V, excitatory glutamatergic inputs to layer VI pyramidal neurons were mildly modulated by nAChRs. As was reported (Kassam et al. 2008), we found that these neurons are modulated by β2* nAChRs that are responsible for the strong activation of the layer VI neuronal population. Layer VI pyramidal neurons in entorhinal cortex also have been reported to be modulated by non-α7 nAChRs, most likely containing β2 subunits (Tu et al. 2009).

Modulation of PFC Interneurons by nAChRs

Interneurons form a highly diverse group of cells with distinct roles in cortical computation (Kawaguchi 1993; Markram et al. 2004). Here, we distinguished between FS and NFS cells, as well as somatostatin-positive cells, a subgroup of NFS cells. FS cells target the perisomatic region of pyramidal neurons (Kawaguchi and Kubota 1997, 2002) and are therefore thought to be involved in regulating the activity window of pyramidal neurons. In somatosensory areas, FS cells regulate feedforward inhibition of incoming thalamic inputs (Sun et al. 2006). Feedforward inhibition in the PFC plays an important role in the integration of hippocampal inputs, which enter the PFC through superficial layers (Jay and Witter 1991; Tierney et al. 2004). We find that FS cells in layer II/III contain α7 nAChRs, as do about half of the FS cells in layer V. This contrasts to studies that report the absence of nAChRs on these neurons, which might be attributable to the use of a different agonist (Couey et al. 2007) or species and age differences (Gulledge et al. 2007). nAChR activation on FS interneurons in PFC layer II/III may alter processing of hippocampal inputs.

Somatostatin-positive cells target distal dendritic regions (Kawaguchi and Kondo 2002; Silberberg and Markram 2007) and can mediate disynaptic inhibition between pyramidal neurons (Kapfer et al. 2007; Silberberg and Markram 2007). We found that all cells that are nonfast-spiking and somatostatin-positive in layers II/III and V were positive for nAChRs, suggesting that nAChRs play an important role in modulating feedback inhibition among pyramidal neurons in these layers.

Increased inhibition through activation of nAChRs expressed by interneurons has been found in many different brain regions (Jones and Yakel 1997; Xiang et al. 1998; McQuiston and Madison 1999; Alkondon et al. 2000; Ji and Dani 2000; Mansvelder et al. 2002; Gulledge et al. 2007). When activated by nAChR stimulation, interneurons can alter activity and plasticity in pyramidal neurons (Xiang et al. 1998; Alkondon et al. 2000; Ji and Dani 2000; Ji et al. 2001; Couey et al. 2007). Increased inhibition can lead to blockade of LTP induction in the hippocampus (Ji et al. 2001) and an increase in the threshold for induction of spike timing–dependent plasticity (Couey et al. 2007). Similar mechanisms may play a role across PFC layers since we find that NFS cells in all layers express nAChRs.

An Integrated View of PFC Neuronal Network Modulation by nAChRs

An understanding of how information processing in cortical networks is altered by nAChR activation requires an integrated view of nAChR activation across all layers, with cellular resolution. Using voltage-sensitive dye imaging, Tu et al. (2009) found that in entorhinal cortex low concentrations of nicotine predominantly activate neuronal populations in layer VI. However, the identity of the activated neurons could not be confirmed during these experiments due to lack of cellular resolution. Two-photon imaging offers cellular resolution while simultaneously monitoring the activity of hundreds of neurons (Cossart et al. 2005). Using this method, we find that in the PFC distinct populations of neurons are activated by nAChR stimulation in a layer-specific manner. As in entorhinal cortex (Tu et al. 2009), we find that in the PFC nAChR stimulation results in the strongest activation of layer VI neuronal populations. These populations consist of both pyramidal neurons and interneurons. A similar picture is seen in layer V, but β2* nAChRs located on presynaptic terminals activate layer V output neurons to a lesser extent than postsynaptic β2* nAChRs in layer VI pyramidal neurons. In contrast, nicotinic AChR-mediated activation of neuronal populations in layer II/III only consisted of interneurons. When monitoring network activity induced by ACh, we found that in all layers, the amount of nAChR-induced neuronal activity in α7-null mice is comparable to that seen in WT mice. In contrast, in layer II/III and V networks of β2-null mice, nAChR-induced neuronal activity is absent. Thus, during bath application of ACh, nicotinic receptor modulation of the activity in PFC layer II/III and V neuronal populations is dominated by β2* nAChRs. We show that α7 nAChRs are not efficiently activated by slow increases in acetylcholine as delivered through bath application. The amplitude of the depolarizing current reached by bath application is low and probably does not induce action potential firing in these cells. β2* receptors are efficiently activated by both types of ACh application. Part of cholinergic signaling in the PFC happens on the scale of seconds to minutes (Sarter et al. 2009). Hence, these data suggest that during prolonged high levels of acetylcholine, the increase in neuronal activity is mainly mediated by β2* nAChRs. For induction of neuronal action potential firing by α7 nAChR stimulation, faster subsecond cholinergic signals may be required.

Changing Levels of nAChR Modulation and Expression over Development

nAChR expression levels change over development. For the PFC, it has been shown that β2* nAChR responses to acetylcholine of LVI pyramidal neurons decrease with age in the PFC (Kassam et al. 2008). Also, α7 nAChRs are known to be highly expressed in developing networks and distribution and expression changes in the developing cortex, but expression persists into adulthood (Tribollet et al. 2004), although this is not specifically known for the PFC. Nicotinic receptors might therefore be involved in the development of neuronal networks. Indeed, α7 nAChRs have indeed been implicated in the formation of thalamocortical synapses (Broide et al. 1996) and β2* nAChRs in the structural development of PFC LVI pyramidal neurons (Bailey et al. 2012). In this study, we used young PFC slices. Nicotinic receptor modulation of the PFC might be altered in adult animals.

Functional Implications

Rapid acetylcholine release is critical for attention performance (Parikh et al. 2007). Nicotine can enhance attention

performance by acting on nAChRs in the PFC (Hahn et al. 2003). Accumulating evidence indicates that β2* nAChRs have a central role in regulating neuronal networks involved in attention. First, specific reexpression of the β2 subunit in β2-null mice increases attention performance (Guillem et al. 2011). Second, diminishing endogenous activation of β2* receptors by deleting its accessory α5 subunit leads to decreased attention performance in the 5-choice serial reaction time task (Bailey et al. 2010). Third, β2* nAChR agonist are more efficient in enhancing cognitive performance in attention tasks compared with nicotine that acts on both β2* and α7 nAChRs (Howe et al. 2010). We found that β2* nAChRs are the main receptor subtype altering activity within the neuronal network of the PFC upon prolonged slow application of ACh. Layer II/III pyramidal neurons are inhibited by nAChR stimulation. Layer V and layer VI pyramidal neurons, which connect to subcortical output structures, get prominently activated by nAChR stimulation. Layer VI pyramidal neurons, which get most prominently activated, project mainly to the medial dorsal thalamus, whereas layer V neurons project mainly to the striatum and hypothalamus (Gabbott et al. 2005). How acetylcholine and nicotine alter prefrontal cortical network activity in different cortical layers during attentional tasks is not known. Our data show that nAChRs regulate prefrontal cortical circuitry in a layer-specific manner. Hence, when studying the modulatory effects of acetylcholine release and nicotine on attention performance in vivo, layer specificity is a critical factor.

Funding

The Netherlands Organisation for Scientific Research (NWO) (917.76.360); VU University Board, Neuroscience Campus Amsterdam; European Research Council to H.D.M.

Notes

The authors wish to thank Prof. Guus Smit and Dr Rhiannon Meredith for valuable comments on the manuscript, Zimbo Boudewijns for exquisite assistance performing Nissl stainings, Prof. Uwe Maskos for sharing α7- and β2-null mice, Prof. Harry Uylings for insightful discussions on analyzing Nissl stainings, Brendan Lodder for Neurolucida reconstructions, and Hans Lodder, Jaap Timmerman, and Tim Heistek for excellent technical assistance.

H.D.M., R.B.P., and B.B. designed the research. R.B.P. performed and analyzed electrophysiological experiments. B.B. performed and analyzed 2-photon experiments. B.S. and J.W. contributed to electrophysiological experiments. C.P.J.K. performed histological staining, R.B.P. analyzed histological staining. R.B.P. and H.D.M. wrote manuscript. *Conflict of Interest* : None declared.

References

Alkondon M, Pereira EF, Eisenberg HM, Albuquerque EX. 2000. Nicotinic receptor activation in human cerebral cortical interneurons: a mechanism for inhibition and disinhibition of neuronal networks. J Neurosci. 20:66–75.

Bailey CD, Alves NC, Nashmi R, De Biasi M, Lambe EK. 2012. Nicotinic alpha5 subunits drive developmental changes in the activation and morphology of prefrontal cortex layer VI neurons. Biol Psychiatry. 71(2):120–128.

Bailey CD, De Biasi M, Fletcher PJ, Lambe EK. 2010. The nicotinic acetylcholine receptor alpha5 subunit plays a key role in attention circuitry and accuracy. J Neurosci. 30:9241–9252.

Broide RS, Robertson RT, Leslie FM. 1996. Regulation of alpha7 nicotinic acetylcholine receptors in the developing rat somatosensory cortex by thalamocortical afferents. J Neurosci. 16:2956–2971.

Cossart R, Ikegaya Y, Yuste R. 2005. Calcium imaging of cortical networks dynamics. Cell Calcium. 37:451–457.

Couey JJ, Meredith RM, Spijker S, Poorthuis RB, Smit AB, Brussaard AB, Mansvelder HD. 2007. Distributed network actions by nicotine increase the threshold for spike-timing-dependent plasticity in prefrontal cortex. Neuron. 54:73–87.

Dalley JW, Cardinal RN, Robbins TW. 2004. Prefrontal executive and cognitive functions in rodents: neural and neurochemical substrates. Neurosci Biobehav Rev. 28:771–784.

Dalley JW, Theobald DE, Bouger P, Chudasama Y, Cardinal RN, Robbins TW. 2004. Cortical cholinergic function and deficits in visual attentional performance in rats following 192 IgG-saporin-induced lesions of the medial prefrontal cortex. Cereb Cortex. 14:922–932.

Disney AA, Aoki C, Hawken MJ. 2007. Gain modulation by nicotine in macaque v1. Neuron. 56:701–713.

Gabbott PL, Warner TA, Jays PR, Salway P, Busby SJ. 2005. Prefrontal cortex in the rat: projections to subcortical autonomic, motor, and limbic centers. J Comp Neurol. 492:145–177.

Gil Z, Connors BW, Amitai Y. 1997. Differential regulation of neocortical synapses by neuromodulators and activity. Neuron. 19:679–686.

Gioanni Y, Rougeot C, Clarke PB, Lepouse C, Thierry AM, Vidal C. 1999. Nicotinic receptors in the rat prefrontal cortex: increase in glutamate release and facilitation of mediodorsal thalamo-cortical transmission. Eur J Neurosci. 11:18–30.

Groenewegen HJ, Uylings HB. 2000. The prefrontal cortex and the integration of sensory, limbic and autonomic information. Prog Brain Res. 126:3–28.

Guillem K, Bloem B, Poorthuis RB, Loos M, Smit AB, Maskos U, Spijker S, Mansvelder HD. 2011. Nicotinic acetylcholine receptor beta2 subunits in the medial prefrontal cortex control attention. Science. 333:888–891.

Gulledge AT, Park SB, Kawaguchi Y, Stuart GJ. 2007. Heterogeneity of phasic cholinergic signaling in neocortical neurons. J Neurophysiol. 97:2215–2229.

Hahn B, Shoaib M, Stolerman IP. 2003. Involvement of the prefrontal cortex but not the dorsal hippocampus in the attention-enhancing effects of nicotine in rats. Psychopharmacology. 168:271–279.

Howe WM, Ji J, Parikh V, Williams S, Mocaer E, Trocme-Thibierge C, Sarter M. 2010. Enhancement of attentional performance by selective stimulation of alpha4beta2(*) nAChRs: underlying cholinergic mechanisms. Neuropsychopharmacology. 35:1391–1401.

Jay TM, Witter MP. 1991. Distribution of hippocampal CA1 and subicular efferents in the prefrontal cortex of the rat studied by means of anterograde transport of Phaseolus vulgaris-leucoagglutinin. J Comp Neurol. 313:574–586.

Ji D, Dani JA. 2000. Inhibition and disinhibition of pyramidal neurons by activation of nicotinic receptors on hippocampal interneurons. J Neurophysiol. 83:2682–2690.

Ji D, Lape R, Dani JA. 2001. Timing and location of nicotinic activity enhances or depresses hippocampal synaptic plasticity. Neuron. 31:131–141.

Jones S, Yakel JL. 1997. Functional nicotinic ACh receptors on interneurones in the rat hippocampus. J Physiol. 504(Pt 3):603–610.

Kapfer C, Glickfeld LL, Atallah BV, Scanziani M. 2007. Supralinear increase of recurrent inhibition during sparse activity in the somatosensory cortex. Nat Neurosci. 10:743–753.

Kassam SM, Herman PM, Goodfellow NM, Alves NC, Lambe EK. 2008. Developmental excitation of corticothalamic neurons by nicotinic acetylcholine receptors. J Neurosci. 28:8756–8764.

Kawaguchi Y. 1993. Groupings of nonpyramidal and pyramidal cells with specific physiological and morphological characteristics in rat frontal cortex. J Neurophysiol. 69:416–431.

Kawaguchi Y, Kondo S. 2002. Parvalbumin, somatostatin and cholecystokinin as chemical markers for specific GABAergic interneuron types in the rat frontal cortex. J Neurocytol. 31:277–287.

Kawaguchi Y, Kubota Y. 1997. GABAergic cell subtypes and their synaptic connections in rat frontal cortex. Cereb Cortex. 7:476–486.

Kawai H, Lazar R, Metherate R. 2007. Nicotinic control of axon excitability regulates thalamocortical transmission. Nat Neurosci. 10:1168–1175.

Lambe EK, Picciotto MR, Aghajanian GK. 2003. Nicotine induces glutamate release from thalamocortical terminals in prefrontal cortex. Neuropsychopharmacology. 28:216–225.

Ma Y, Hu H, Berrebi AS, Mathers PH, Agmon A. 2006. Distinct subtypes of somatostatin-containing neocortical interneurons revealed in transgenic mice. J Neurosci. 26:5069–5082.
Mansvelder HD, Keath JR, McGehee DS. 2002. Synaptic mechanisms underlie nicotine-induced excitability of brain reward areas. Neuron. 33:905–919.
Mansvelder HD, McGehee DS. 2000. Long-term potentiation of excitatory inputs to brain reward areas by nicotine. Neuron. 27:349–357.
Markram H, Toledo-Rodriguez M, Wang Y, Gupta A, Silberberg G, Wu C. 2004. Interneurons of the neocortical inhibitory system. Nat Rev. 5:793–807.
McGehee DS, Role LW. 1995. Physiological diversity of nicotinic acetylcholine receptors expressed by vertebrate neurons. Annu Rev Physiol. 57:521–546.
McQuiston AR, Madison DV. 1999. Nicotinic receptor activation excites distinct subtypes of interneurons in the rat hippocampus. J Neurosci. 19:2887–2896.
Nicoll A, Kim HG, Connors BW. 1996. Laminar origins of inhibitory synaptic inputs to pyramidal neurons of the rat neocortex. J Physiol. 497(Pt 1):109–117.
Parikh V, Kozak R, Martinez V, Sarter M. 2007. Prefrontal acetylcholine release controls cue detection on multiple timescales. Neuron. 56:141–154.
Passetti F, Dalley JW, O'Connell MT, Everitt BJ, Robbins TW. 2000. Increased acetylcholine release in the rat medial prefrontal cortex during performance of a visual attentional task. Eur J Neurosci. 12:3051–3058.
Penschuck S, Chen-Bee CH, Prakash N, Frostig RD. 2002. In vivo modulation of a cortical functional sensory representation shortly after topical cholinergic agent application. J Comp Neurol. 452:38–50.
Poorthuis RB, Goriounova NA, Couey JJ, Mansvelder HD. 2009. Nicotinic actions on neuronal networks for cognition: general principles and long-term consequences. Biochem Pharmacol. 78:668–676.
Porter JT, Cauli B, Tsuzuki K, Lambolez B, Rossier J, Audinat E. 1999. Selective excitation of subtypes of neocortical interneurons by nicotinic receptors. J Neurosci. 19:5228–5235.
Sarter M, Parikh V, Howe WM. 2009. Phasic acetylcholine release and the volume transmission hypothesis: time to move on. Nat Rev. 10:383–390.
Silberberg G, Markram H. 2007. Disynaptic inhibition between neocortical pyramidal cells mediated by Martinotti cells. Neuron. 53:735–746.
Sun QQ, Huguenard JR, Prince DA. 2006. Barrel cortex microcircuits: thalamocortical feedforward inhibition in spiny stellate cells is mediated by a small number of fast-spiking interneurons. J Neurosci. 26:1219–1230.
Tierney PL, Degenetais E, Thierry AM, Glowinski J, Gioanni Y. 2004. Influence of the hippocampus on interneurons of the rat prefrontal cortex. Eur J Neurosci. 20:514–524.
Trevelyan AJ, Sussillo D, Watson BO, Yuste R. 2006. Modular propagation of epileptiform activity: evidence for an inhibitory veto in neocortex. J Neurosci. 26:12447–12455.
Tribollet E, Bertrand D, Marguerat A, Raggenbass M. 2004. Comparative distribution of nicotinic receptor subtypes during development, adulthood and aging: an autoradiographic study in the rat brain. Neuroscience. 124:405–420.
Tu B, Gu Z, Shen JX, Lamb PW, Yakel JL. 2009. Characterization of a nicotine-sensitive neuronal population in rat entorhinal cortex. J Neurosci. 29:10436–10448.
Van De Werd HJ, Rajkowska G, Evers P, Uylings HB. 2010. Cytoarchitectonic and chemoarchitectonic characterization of the prefrontal cortical areas in the mouse. Brain Struct Funct. 214:339–353.
Xiang Z, Huguenard JR, Prince DA. 1998. Cholinergic switching within neocortical inhibitory networks. Science. 281:985–988.
Young JW, Crawford N, Kelly JS, Kerr LE, Marston HM, Spratt C, Finlayson K, Sharkey J. 2007. Impaired attention is central to the cognitive deficits observed in alpha 7 deficient mice. Eur Neuropsychopharmacol. 17:145–155.